Published online July 22, 2004

3864–3876 *Nucleic Acids Research, 2004, Vol. 32, No. 13*
doi:10.1093/nar/gkh722

New invMED1 element *cis*-activates human multidrug-related *MDR*1 and *MVP* genes, involving the LRP130 protein

Stéphane Labialle, Guila Dayan, Landry Gayet, Dominique Rigal[1], Joël Gambrelle[2] and Loris G. Baggetto*

Institut de Biologie et Chimie des Protéines (IBCP UMR5086 CNRS UCBL), 7 Passage du Vercors, F-69367 Lyon Cedex 07, France, [1]EFS Lyon, 1 passage du Vercors, F-69007 Lyon, France and [2]Service d'Ophtalmologie, Hôpital de la Croix-Rousse, 103 Gde rue de la Croix-Rousse, F-69317 Lyon Cedex 04, France

Received April 19, 2004; Revised and Accepted July 8, 2004

ABSTRACT

The *MDR*1 gene is a key component of the cytotoxic defense network and its overexpression results in the multidrug resistance (MDR) phenotype. However, the molecular mechanisms that regulate the *MDR*1 gene and coordinate multiple MDR-related genes expression are poorly understood. In a previous study, we identified a new 12 bp *cis*-activating region in the 5′-flanking region of the human MDR1 gene, which we called inverted MED1. In the present study, we characterized the precise binding element, which we named invMED1, and revealed the presence of the LRP130 protein as the nuclear factor. Its binding intensity increases with the endogenous *MDR1* gene expression and with the MDR level of CEM leukemia cells. Interestingly, the LRP130 level did not vary with the chemoresistance level. We observed the involvement of LRP130 in the transcriptional activity of the *MDR*1 gene promoter, and moreover, in that of the MDR-related, invMED1-containing, *MVP* gene promoter. We used siRNAs and transcriptional decoys in two unrelated human cancer cell lines to show the role of the invMED1/LRP130 couple in both *MDR*1 and *MVP* endogenous genes activities. We showed that invMED1 was localized in the −105/−100 and −148/−143 regions of the *MDR*1 and *MVP* gene promoters, respectively. In addition, since the invMED1 sequence is primarily located in the −160/−100 bp region of mammalian MDR-related genes, our results present the invMED1/LRP130 couple as a potential central regulator of the transcription of these genes.

INTRODUCTION

One of the most investigated mechanisms of multidrug resistance (MDR) is drug efflux mediated by carriers with a broad substrate specificity. It results mainly from the overproduction of P-glycoprotein (Pgp), a transmembrane protein that belongs to the ATP-binding cassette (ABC) transporter superfamily. Pgp is encoded by the *MDR*1 gene in human and by *mdr*1a and *mdr*1b genes in rodents. ABC transporters utilize energy from ATP hydrolysis to transport a large variety of substrates including chemotherapeutic drugs across biological membranes. Other ABC transporters such as the multidrug resistance-associated proteins MRP1, MRP2, MRP3, MRP4 and MRP5 (1–5), and the breast cancer resistance protein, BCRP (6), also named MXR (mitoxantrone resistance), may be overproduced alone or in any combination by chemoresistant cells. MDR3, a protein closely related to Pgp, acts as a phosphatidylcholine translocase and may also be involved in drug transport (7–9).

Although the lung resistance protein (LRP) is not an ABC transporter, it is involved in the MDR phenotype as the expression of its gene closely reflects the chemoresistance profile of many cancer cell lines and tumors. LRP was found to be identical to the major vault protein (MVP) (10) and makes up >70% of the total mass of the vault complex, a large-sized ribonucleoprotein found mostly in the cytoplasm (11) and in the nucleus (12,13). Vaults are present with high levels in tissues chronically exposed to xenobiotics and may mediate multidrug resistance by transporting drugs away from their intracellular targets or by transporting them to exocytic vesicles or efflux pumps (14). In several clinical studies, but not all, increased MVP expression is associated in general with a higher level of drug resistance analyzed *in vitro* by flow cytometry (15,16). Interestingly, in acute myeloid leukemia, the worst response and/or survival rate to the treatment was observed in patients who co-expressed MVP and Pgp (17–20). Moreover, in breast cancer, *MVP* expression, as well as *MDR*1 expression, have been correlated to the presence of nodal metastasis (21).

MDR-related genes share some common features concerning their transcriptional regulation. Human genes examined to date lack a TATA box, while other rodents homologs are TATA-dependent. In human, an initiator element (INR) has been functionally described in the *MDR*1 promoter and near-consensus INR sequences are present within the promoters of *MRP*2 and *BCRP* genes. Like most other TATA-less genes, MDR-related genes generally possess both CCAAT box and GC-rich elements for their constitutive transcription. Tumor

*To whom correspondence should be addressed. Tel: +33 0 4 72 72 26 35; Fax: +33 0 4 72 72 26 26; Email: lg.baggetto@ibcp.fr

suppressor and oncogene-responsive elements are also present, explaining the high level of expression often observed in drug-naive tumors. For example, *MDR*1, *MRP*1 and probably *MVP* human genes contain a p53 element. In addition, these genes together with MRP2 also contain an AP-1 element.

However, few data have been reported to date on an eventual link between regulatory elements specifically relevant to multidrug resistance and the transcription of MDR-related genes. Those that are available require confirmation, as this is the case for MEF1 (22,23) and SXR binding elements (24). The latter seems to be the most interesting at the moment since it is present in human *MDR*1 and *MRP*3 genes (and also in the rat *MRP*2 homolog), and is thought to coordinate the regulation of drug metabolism and efflux, through co-activation of MDR-related and CYP3A4 genes (24).

In previous studies, we identified a 12 bp region spanning the −108 to −97 bp sequence of the human *MDR*1 gene and suggested the presence of a transcriptional activator element in this region (25); we reported the possible link that could exist between this region, which specifically binds an unknown factor, and the level of chemoresistance (26). Here, we characterized the *cis*-element/*trans*-acting factor couple involved and investigated its relation to the MDR phenotype. We precisely localized the *cis*-activating element at position −105/−100, which we named invMED1, and identified the LRP130 protein as a component of the nuclear factor that binds this element. We demonstrated that the invMED1/LRP130 complex formation increased with the chemoresistance level. We searched for the presence of the invMED1 sequence in MDR-related genes, and localized it in human *MDR*1 and *MVP* genes. Moreover, we have shown that an accurate transcriptional activity for both of them depends on the presence of the LRP130 protein. Finally, the presence of the invMED1 sequence in the −160/−100 region of several MDR-related genes in human and rodents suggests that the invMED1/LRP130 couple could be a possible central regulator of these MDR-related genes.

MATERIALS AND METHODS

Chemicals

Cell culture medium (RPMI-1640), fetal calf serum (FCS), antibiotic and antimycotic solution (containing 10 000 IU/ml penicillin, 10 mg/ml streptomycin and 25 μg/ml amphotericin B), trypsin–ethylene diamine tetraacetic acid (EDTA) and phosphate-buffered saline (PBS) were from Sigma (St Quentin Fallavier, France). Vinblastine, prepared in water under sterile conditions and sterile-filtered, was a gift from Roger Bellon Laboratories (Neuilly sur Seine, France). The synthetic peptide MPG was synthesized and analyzed as previously described (27) and was reported to be non-immunogenic.

Oligodeoxynucleotides

All oligodeoxynucleotides were purchased from Sigma-Genosys. Double-stranded oligodeoxynucleotides (ODNs) used in electrophoresis experiments were cyanine-5-labeled. When used for transfection experiments, ODNs were phosphorothioate-modified on the first base at the 5′ end and on the two last bases at the 3′ end. In each case, double-stranded ODNs were formed by annealing an equimolar mixture of sense and antisense single-stranded ODNs in 10 mM Tris–HCl, pH 8.0, and 1 mM EDTA by heating for 5 min at 70°C, followed by slow cooling at room temperature.

Cell culture and viability

Human lymphoblastic leukemia CEM cell lines were maintained in RPMI-1640 medium (Sigma) supplemented with 10% FCS, antibiotic and antimycotic solution (1 ml per 100 ml medium) to make a complete medium. Cells were grown at 37°C in a humidified atmosphere containing 5% CO_2. The highly drug-resistant cell lines, CEM/VLB0.45 and CEM/VLB5, were established by growing the corresponding sensitive parental cell line in medium containing stepwise-increasing concentrations of vinblastine as previously described (28). Cells thus selected grow in the presence of 0.45 μg/ml vinblastine for CEM/VLB0.45, and 5 μg/ml vinblastine for CEM/VLB5. Human ciliary body IPC227 and fibrosarcoma HT1080 cell lines were grown at 37°C in a humidified atmosphere containing 5% CO_2, in MEM medium (Sigma) supplemented with 10% FCS, antibiotic and antimycotic solution. All cell lines were regularly checked for mycoplasma contamination with both MycoTect (Gibco-BRL Life Technologies, Cergy Pontoise, France) according to the manufacturer's instructions and by fluorescence staining with Hoechst 33258 (Sigma France). Cell viability was measured by exclusion of Trypan blue (Sigma France).

Plasmid constructions

Reporter constructs. An *MDR1* promoter fragment (−197 to +151 with respect to the major +1 transcriptional start site) was amplified by PCR from pSV00CAT/pMDR1h (a generous gift from Dr M. M. Gottesman) using primers designed to create NheI and HindIII restriction sites (TATGCTAGCTAGAGAGGTGCAAC and TATAAGCTTACCTCGCGCT) and was inserted into the pGL2-Basic reporter vector (Promega) to give the pGL2-hMDR1 construct. In order to delete the 6 bp invMED1 sequence of the promoter, two fragments were amplified by PCR from pSV00CAT/pMDR1h with the following primers: TATGCTAGCTAGAGAGGTGCAAC and GGCCCGGATTGACTGAATG for the first 101 bp fragment and AGTCATCTGTGGTGAGGCTG and TATAAGCTTACCTCGCGCT for the second 241 bp fragment. The two fragments were restricted with NheI and HindIII, respectively, then ligated via their blunt ends with T4 DNA ligase (Promega France). Finally, both constructs were inserted into pGL2-Basic to give the plasmid pGL2-hMDR1-ΔinvMED1.

An *MVP* promoter fragment (−1859 to +23) was isolated from pCR-MVP1.9 (a generous gift from Dr U. Stein) using KpnI and XhoI and inserted into pGL2-Basic to give the plasmid pGL2-MVP1.9. All constructs were verified by sequencing (Genome Express, France).

Vector construction for LRP130 siRNA expression. A pSilencer-LRP130 construct was made with the pSilencer 2.0-U6 plasmid (Ambion) using the following annealed oligonucleotides: GATCCCCTATAAGAGATGTCCTAATTCAAGAGATTAGGACATCTCTTATAGGTTTTTTGGAAA and AGCTTTTCCAAAAAACCTATAAGAGATGTCCTAATCTCTTGAATTAGGACATCTCTTATAGGGG. This

construct targeted the AACCTATAAGAGATGTC sequence located from position 1708 to 1729 in the LRP130 mRNA.

Transfection experiments

Transient cell transfection. All plasmids were purified using the Endofree Plasmid Maxi kit (Qiagen, Courtaboeuf, France) according to the manufacturer's instructions. CEM cells (10^6/ml) were placed into 1 ml of unsupplemented RPMI-1640 culture medium. A mixture consisting of 1.5 μg of the plasmid of interest, 0.5 μg of pSV-β-Galactosidase and 4 μl of the transfection agent Tfx-20 per microgram of DNA (Promega France) was added dropwise to the cells and incubated for 1 h at 37°C before the addition of 5 ml of supplemented RPMI-1640 medium, according to the manufacturer's instructions. Luciferase and β-galactosidase enzymatic activities were detected after 48 h of incubation at 37°C using the Dual-Light luciferase and β-galactosidase reporter gene assay system kit (Tropix, Bedford, MA, USA) and an MLX Microtiter Plate Luminometer (Dynex Technologies). The pSV-β-Galactosidase vector was used as an internal positive control to monitor transfection efficiency. We used the pGL2-control vector (Promega) as the positive expression control.

HT1080 cells were transfected with either the pSilencer-LRP130 plasmid or the pSilencer-negative control furnished by the manufacturer. A mixture of 2 μg of plasmid and 6 μl of Lipofectamine-2000 was added dropwise to 10^6 cells and incubated for 4 h before the change of the medium by supplemented MEM medium, according to the manufacturer's instructions.

ODN transfer into target cells. Highly chemoresistant CEM/VLB5 cells (3×10^6 cells) that had been cultured for at least 1 week in the absence of vinblastine were washed twice in PBS buffer and transfected by the Nucleofector™ technology (Amaxa Biosystems) in the presence of 3 μg of phosphorothioate-modified double-stranded ODNs. We used Cell Line Kit R and protocol T-20 for transfection. Cells were then incubated for 3 days in complete culture medium before total RNA purification and RT–PCR experiments.

For ODN transfer in the weakly chemoresistant IPC227 cell line, 0.7×10^6 cells were washed twice in PBS buffer and incubated for 3 h in the presence of 25 μM of a combination of MPG (27) and phosphorothioate-modified double-stranded ODNs in a 25:1 molar ratio. Cells were then incubated for 3 days in supplemented medium.

Total RNA extraction and cDNA amplification

Total RNA was prepared from cultured cell lines using the RNeasy starter kit (Qiagen) and cDNA was synthesized from 1 μg of total RNA. Reverse transcription was carried out by the use of M-MLV Reverse Transcriptase, Point Mutant and oligo$(dT)_{15}$ primers (Promega France), according to the manufacturer's instructions. After reverse transcription, RNAse H Minus (Promega France) was added.

cDNA amplification was carried out by PCR using *Taq* DNA polymerase (Sigma France) and the following specific oligodeoxynucleotide probes: AGAAGTGATATCAATGATACAGGGTTC and GTTGCCATTGACTGAAAGAACA for *MDR*1; TTTGATGTCACAGGGCAAGTT and GTCCACCAAATCCAGAACCTC for *MVP*; GAGGGTAACCAGGAAGTTCCG and ATCGTTCAGTGTGAAGCCCTTG for *LRP130*; GACTGGCAGGGCTACTTCTACA and GTCTTGGTCTTCATCGCCAT for *MRP*1; TCCTATGTGGGCGACGAG and GATGGGCACAGTGTGGGT for β-*actin*; CCAAAGTTGTCATGGATGACC and GTGGATATTGTTGCCATCAATG for *GAPDH*. PCR consisted of an initial denaturation step at 94°C for 4 min, followed by 30 cycles at 94°C for 1 min, annealing at 60°C for 45 s for all probes, and extension at 72°C for 1 min in each cycle. The resulting PCR products were 314, 429, 309, 429, 342 and 425 bp long for *MDR*1, *MVP, LRP130, MRP*1, β-*actin* and *GAPDH*, respectively.

Preparation of nuclear proteins

We used the method described by Jackson (29) with the following modifications: 10^9 cells were centrifuged at 980 *g* for 5 min at 4°C and washed twice in PBS. All the following steps were performed at 4°C and all subsequent buffers contained a protease inhibitor cocktail composed of 1 mM phenylmethanesulfonyl fluoride, 1 mM sodium metabisulfite and 1 mM dithiothreitol. The pellet was suspended twice in 80 ml PBSM buffer (137 mM NaCl, 2.7 mM KCl, 6.5 mM anhydrous Na_2HPO_4, 1.5 mM KH_2PO_4, 4.9 mM $MgCl_2$, pH 6.6) and centrifuged at 4600 *g* for 15 min. The pellet was suspended in five estimated packed-cell volumes of buffer A (10 mM HEPES–KOH, pH 7.6, 1.5 mM $MgCl_2$, 10 mM KCl) and incubated for 20 min at 4°C. After centrifugation at 2800 *g* for 10 min, the pellet was suspended in two estimated packed-cell volumes of buffer A and homogenized in a Potter–Elvehjem with 15 up- and-down strokes. The mixture was centrifuged at 2800 *g* for 10 min, and the pellet containing the nuclei was gently resuspended in 80 ml of buffer B (20 mM HEPES–KOH, pH 7.6, 25% glycerol, 420 mM NaCl, 0.2 mM EDTA, 5 mM $MgCl_2$) on a slow-motion rocking platform for 30 min. After centrifugation at 21 000 *g* for 30 min, the volume of the supernatant was measured. While the supernatant was being agitated, 0.33 g/ml ammonium sulfate powder was slowly added over 10 min, followed by the addition, over 10 min, of 4 μl of 10 M KOH for every gram of ammonium sulfate added. The mixture was agitated for 45 min, and the precipitated nuclear proteins were collected by centrifugation at 21 000 *g* for 15 min. The pellet was suspended in 600 μl buffer C (20 mM HEPES–KOH, pH 7.6, 20% glycerol, 50 mM KCl, 0.2 mM EDTA, 5 mM $MgCl_2$). This mixture was dialyzed three times against 500 ml buffer C. Insoluble fragments were removed by centrifugation at 10 000 *g* for 10 min. Proteins were stored at −80°C.

Separation of nuclear proteins

Heparin–sepharose affinity chromatography. Nuclear proteins were separated by heparin–sepharose affinity chromatography using a HiTrap Heparin HP column (Amersham Pharmacia) mounted in a Biorad Biologic LP chromatography system at a flow rate of 0.25 ml/min. Total nuclear proteins (2 mg) were loaded on to the column in the following low-salt buffer: 20 mM HEPES–KOH pH 7.6, 20% glycerol, 50 mM KCl, 0.2 mM EDTA, 5 mM $MgCl_2$. Bound proteins were eluted by stepwise increases in KCl concentration from 0.1 to 1 M, monitoring UV absorbance at 280 nm. Eluted proteins were dialyzed using 3500 MWCO Slide-A-Lyzer cassettes (Pierce), against the low salt buffer.

DNA-affinity chromatography. We used the μMACS Streptavidin Kit (Miltenyi Biotec). Briefly, 5′ biotin-labeled $[GGGAGC]_8$ ODNs were incubated with nuclear proteins as described in the Nuclear protein analysis section. The mixture was then incubated with magnetic streptavidin microbeads. Protein separation was done in a microcolumn placed in a magnetic field. Washing steps were applied with the same binding buffer as that for the protein–ODN interaction. Specifically interacting molecules were eluted with the binding buffer containing increasing concentrations of KCl (0.5 to 2 M). Verification of total protein elution was checked by removing the column from the magnetic field before applying the first elution buffer.

Protein assay

Protein concentrations were measured by the Bradford method (30) using the BCA protein assay reagent kit (Pierce) according to the manufacturer's instructions.

Nuclear protein analysis

Nuclear protein–ODN interaction. Nuclear proteins (5–15 μg) were incubated with 1 μmol cyanine-5-labeled ODN in a total volume of 30 μl in the presence of 5 μg acetylated bovine serum albumin (Promega) and 0.5 μg of poly(dI–dC) in the binding buffer (25 mM Tris–HCl, pH 7.5, 50 mM KCl, 1 mM DTT, 5% glycerol) for 25 min at 30°C in the dark.

UV cross-linking. The nuclear protein–ODN complex was cross-linked by exposure to UV radiation at 250 nm for 30–60 min in the dark.

Sodium dodecyl sulfate–polyacrylamide gel electrophoresis. Protein samples were analyzed by SDS–PAGE in 6 to 10% polyacrylamide gels using the following loading buffer: 100 mM Tris–HCl, pH 6.8, 200 mM dithiotreitol, 0.2% bromophenol blue, 4% SDS and 20% glycerol, as described by Laemmli (31) and detailed previously (32). Gels were stained either with Coomassie Brillant Blue G-250 or with silver using the SilverQuest silver staining kit (Invitrogen), and cyanine-5 fluorescence was detected using a STORM 860 densitometer (Molecular Dynamics, Amersham-Pharmacia-Biotech, Orsay, France).

Electromobility shift assay. Gel retardation experiments were carried out on 9% acrylamide/bis-acrylamide (19:1), 2.5% glycerol gels (Sigma France) in running buffer (25 mM Tris–base, 192 mM glycine, 2 mM EDTA, pH 8.3), at 150 V for 4 h in a refrigerated chamber at 4°C in the dark. The gels were scanned for cyanine-5 fluorescence as described above.

Mass spectrometry. Coomassie blue- or cyanine-5-stained bands were subjected to in-gel tryptic digestion using modified porcine trypsin (Promega, Madison, WI). Tryptic digests were analyzed by online capillary high-performance liquid chromotography (HPLC) (LC Packings, Dionex, Amsterdam, The Netherlands) coupled to a nanospray LCQ Deca ion trap mass spectrometer (ThermoFinnigan, San Jose, CA, USA). Peptides were separated on a 75 μm ID × 15 cm PepMap C18 column (LC Packings) after loading onto a 300 μm ID × 5 mm PepMap C18 precolumn. The flow rate was 150 nl/min. Peptides were eluted using a 0–40% linear gradient of solvent B in 40 min (solvent A was 0.1% formic acid in 5% acetonitrile, and solvent B was 0.1% formic acid in 90% acetonitrile). The mass spectrometer was operated in positive ion mode at a 1.9 kV needle voltage and a 30 V capillary voltage. Data acquisition was carried out in a data-dependent mode consisting of, alternatively in a single run, a full scan MS over the range *m*/*z* 370–2000, and a full scan MS/MS in an exclusion dynamic mode. MS/MS data were collected using a three *m*/*z* unit isolation window and a relative collision energy of 35%. The SEQUEST Browser software was used for protein identification from SwissProt and NCBInr databases using the MS/MS spectra.

RESULTS

Characterization of the precise nuclear factor-binding site in the −108/−97 region of the *MDR*1 gene promoter

We have previously shown that the −108/−97 promoter region of the human *MDR*1 gene was able to bind a nuclear protein, the precise boundaries and the nature of which were not defined (25,26).

In order to characterize precisely the boundaries of the nuclear factor-binding site in the −108/−97 DNA region of the *MDR*1 gene sequence, we carried out EMSA experiments using nuclear extracts from human leukemia CEM cells and labeled oligodeoxynucleotides of various lengths as probes. The retarded band that we previously detected with the 12 bp ODN still occurred with a 6 bp ODN centered on the −108/−97 promoter region (ODN6), but was lost when 5 bp ODNs (ODN5A and ODN5B) were used (Figure 1A). When 6 bp ODNs spanning a 10 bp window centered on the −108/−97 region were used, we showed that the only ODN that was involved in nuclear factor binding was ODN6 (Figure 1B), the mutation of which completely abrogated the binding (Figure 1C). The multiple bands seen in Figure 1B corresponded to non-specific binding or were specific to other factors whose binding elements could overlap invMED1; but they disappeared to the benefit of the invMED1/LRP130 couple interaction when the reaction was carried out in the presence of ODN12 (Figure 1A).

In order to determine whether the invMED1 flanking bases modified the binding of the nuclear factor, 6 bp ODNs were substituted at their first, last or both bases (ODN6L, ODN6R, ODN6LR, Figure 1D). In all cases, no retarded band could be detected. In addition, use of 8 or 10 bp ODNs (ODN8 and ODN10) did not significantly change the binding pattern when compared with that of ODN6. Moreover, when one or two extreme bases of these ODNs were substituted (ODN8LR and ODN10LR), no significant change was seen in the retardation pattern. These results suggest that the binding site for a nuclear factor on the −108/−97 region of the human *MDR*1 gene promoter is the actual invMED1 GGGAGC sequence, at position −105/−100.

It is interesting to note that we have found the same retarded band with the same characteristic retardation pattern in several other cell lines such as primary cultures of NHF skin fibroblasts, HepG2 hepatocarcinoma, HT-1080 skin fibrosarcoma, HeLa cervix carcinoma cell line, MCF7 breast adenocarcinoma, A549 lung carcinoma and IPC227 uveal (ciliary body) melanoma and others shown in Figure 2, while we

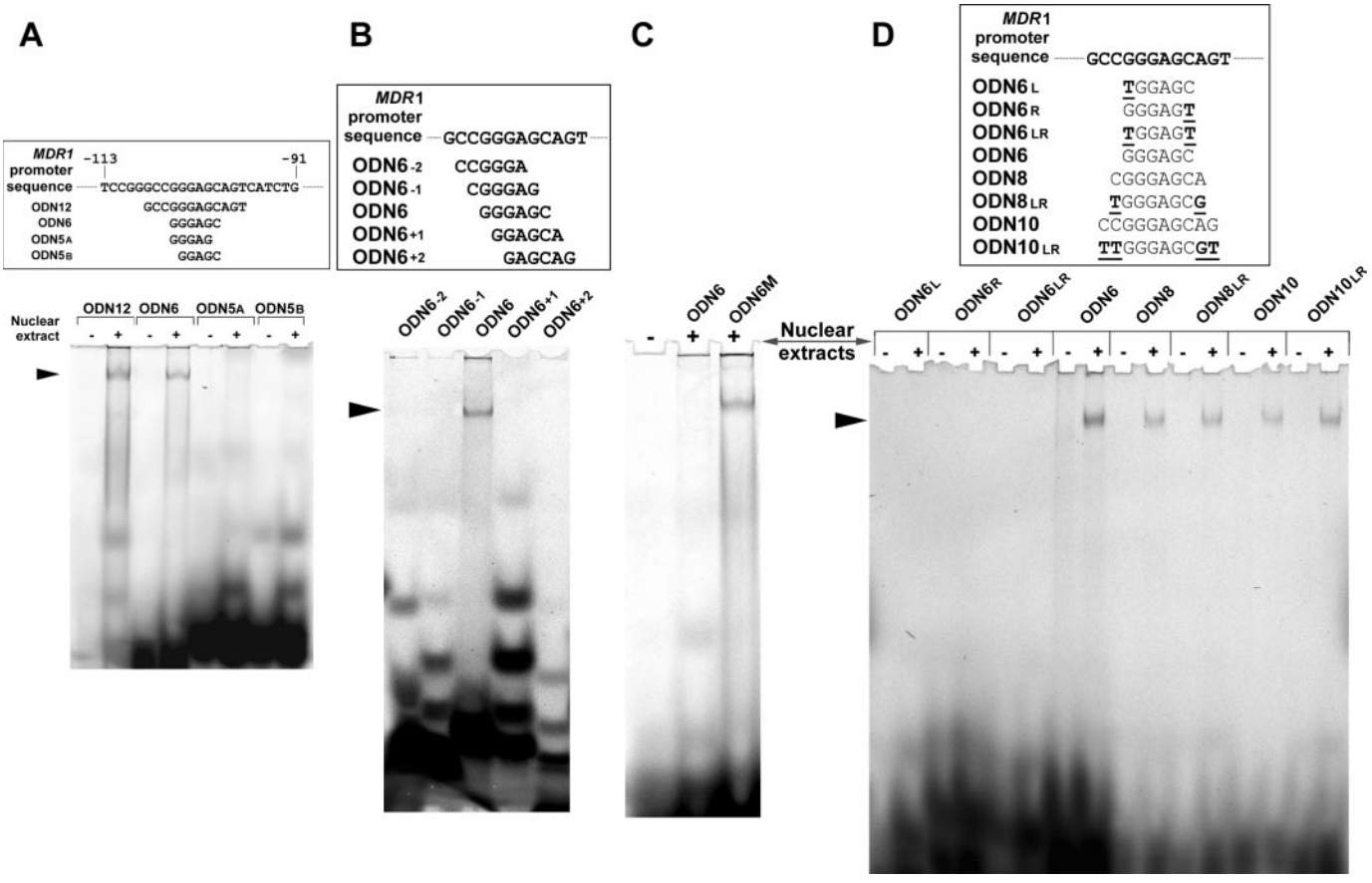

Figure 1. Characterization of the nuclear protein(s)-binding site in the inverted MED-1 DNA region. (**A**) Nuclear extracts from CEM/VLB5 resistant cells were prepared and incubated with labeled ODNs, the sense strand sequence of which is given in the table above the figure, prior to EMSA analysis. The position of each ODN relative to the 5′ regulatory sequence of the *MDR1* gene is given in the DNA fragment at the top of the table. The invMED1 sequence is underlined. The major retarded DNA-protein(s) complex is indicated by an arrowhead. (**B**) Several 6 bp ODNs indicated in the table and spanning a 10 base window centered on the inverted MED-1 sequence were tested for nuclear protein(s) binding. (**C**) EMSA experiments were performed with mutated ODN6M (third G→A substitution) in the absence or the presence of nuclear extracts as compared to ODN6. (**D**) Several 6, 8 and 10 bp ODNs centered on the invMED1 sequence and bearing one or more bases substituted at their ends (bold and underlined characters) from the actual sequence represented on the top of the table, were tested.

did not find it in other uveal melanomas such as the human MU2 choroidal melanoma.

Presence of the invMED1 DNA sequence in promoter regions of MDR- and non-MDR-related genes

The characterization of the precise sequence of the invMED1 element allowed us to search for its presence in other MDR-related gene promoters. Table 1 shows that the invMED1 sequence is present in 7 out of 16 human and rodent MDR-related gene promoters cloned to date. Interestingly, positions of these sequences in promoters are closely located in the −160/−100 region of these genes.

To calculate the occurrence of the invMED1 element, we analyzed the 1869 non-MDR-related human promoters that are deposited in the Eukaryotic Promoter Database (http://www.epd.isb-sib.ch/). Among these, 609 (32.5%) contained at least one invMED1 occurrence (most of the occurrences being partitioned between 1 in 449 promoters, 2 in 160 promoters and 3 in 24 promoters), for a total number of 900 occurrences in their −499/+100 bp window relative to the +1 transcription start site.

The distribution of the A, C, G and T nucleotides out of the 600 bp for each promoter does not follow a random probability of 0.25 per nucleotide. Indeed, as shown in Figure 3A, the [C,G] percentage increases regularly from −499 to +100 to reach 33% for G and 31% for C.

The theoretical probability of having one invMED1 occurrence would be 0.25^6. Knowing that the invMED1 sequence is rich in GC (GGGAGC), and taking into account the nucleotide distribution between −499 and +100, the probability of having an occurrence regularly increases from 0.00029 to 0.00067 and reaches a maximum of 0.00065 between the +1 and +100 region (Figure 3B). One should thus expect to find a higher frequency of occurrences at position −99/+100 than elsewhere. However, the observed/theoretical ratio for the invMED1 occurrence shows that the latter is more frequent in the −299/−100 window relative to the +1 start point. This result is consistent with our finding of invMED1 sequence in both *MDR*1 and *MVP* genes at positions −105/−100 and −148/−143, respectively. The same observation could be made with non-MDR-related rodent genes: 28% and 24.4% of the deposited 196 mouse and 119 rat promoters, respectively, contained at least one GGGAGC occurrence in the

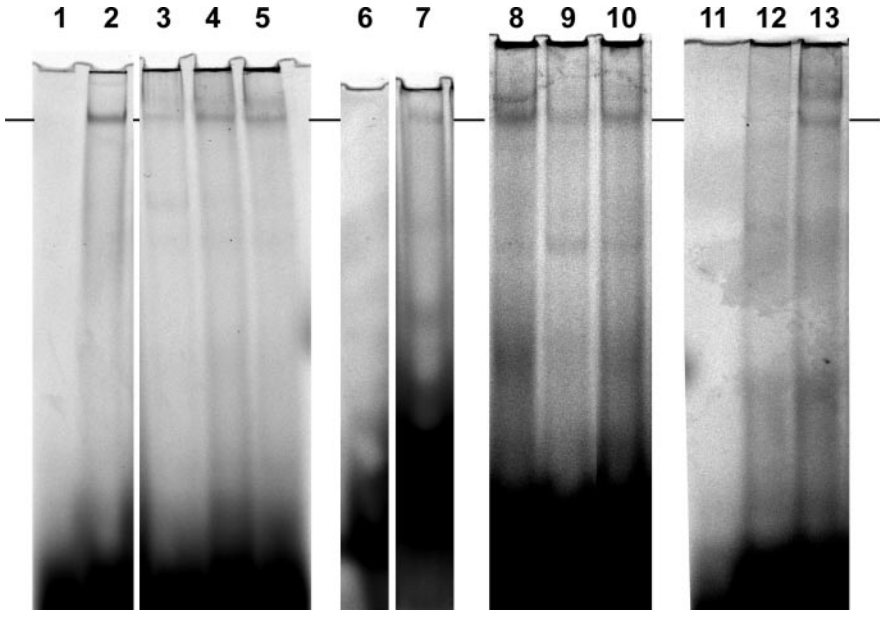

Figure 2. Presence of the invMED1/nuclear factor complex in several cancer and non-cancerous cell lines as revealed by EMSA experiments. Lanes 1, 6, 11: free ODN6; 10 μg of nuclear protein extracts from the following cell lines were deposited in each lane: HepG2 human hepatocellular carcinoma (lane 2), NHF primary human skin fibroblasts (lane 3), KB3.1 human cervix carcinoma (HeLa derivative) (lane 4), MCF7 human breast adenocarcinoma (lane 5), IPC227 human ciliary body melanoma (lane 7), AS30-D/COL10 rat hepatocarcinoma (lane 8), NIH3T3 mouse fibroblast (lane 9), NIH80 mouse NIH3T3 transduced with the human *MDR*1 gene (lane 10), MU2 human epithelioid-type choroidal melanoma (lane 12), HT1080 human skin fibrosarcoma (lane 13). The horizontal line points to the retarded band of interest.

Table 1. Presence and position of the invMED1 sequence in cloned promoters of MDR-related genes in human, mouse and rat

Species	Gene name	Position of the invMED1 sequence
Human	*MDR*1	−105/−100
	*MRP*1	Absent
	*MRP*2	Absent
	*MRP*3	Absent
	BCRP	Absent
	MVP	−148/−143
	*MDR*3	−161/−156
Mouse	*mdr1*a	−108/−103
	*mdr1*b	Absent
	*MRP*1	−130/−125
	MVP	Absent
Rat	*mdr1*b	Absent
	*MRP*1	−122/−117
	*MRP*2	Absent
	*MRP*3	Absent
	*MDR*2	−156/−151

The position of the sequences is given relative to the +1 transcription start site.

−499/+100 region. Taking into account the nucleotide distribution, the observed/theoretical frequency was 1.9 in the −199/−100 region of mouse promoters, and 1.8 and 2.1 in the −299/−200 and −199/−100 regions of rat promoters, respectively.

Interaction of the nuclear factor with the invMED1 DNA sequence as a function of the chemoresistance level of CEM cells

Using the chemosensitive CEM parental cell line and its CEM/VLB0.45, CEM/VLB5 and CEM/VLB10 chemoresistant derivatives, we investigated the nuclear factor-binding capacity to invMED1 as a function of the chemoresistance level. In these cell lines, overexpression of the *MDR*1 gene was the sole mechanism of MDR that we were able to determine (28). We observed a correlation between the increasing level of expression of the MDR phenotype, the increasing *MDR*1 mRNA levels (Figure 4A), and the invMED1 binding intensity (Figure 4B and C). This result suggests that the invMED1 binding capacity of the specific nuclear factor depends on the cellular level of the MDR phenotype. Interestingly, the LRP130 production levels in chemoresistant CEM cells did not significantly vary relative to the parental sensitive cells, as shown in Figure 4D.

Characterization of the invMED1 binding factor

In order to characterize the nuclear protein(s) that binds to the invMED1 sequence, total nuclear proteins were fractionated by heparin–sepharose chromatography with increasing KCl concentrations. Figure 5A shows that the retarded band of interest could be detected in the second peak of the 0.41 M KCl-eluted fraction, suggesting that this fraction contained the invMED1 binding protein(s).

SDS–PAGE was then carried out after UV cross-linking of nuclear proteins from the 0.41 M KCl fraction and invMED1 ODN (Figure 5B). The data showed a single labeled band with an apparent molecular weight of ∼150 kDa. To further characterize the protein content of the labeled band, the latter was analyzed by nano-liquid-chromatography coupled with MS–MS spectrometry, because of the very small amount of protein available. Twelve peptides were retrieved (Table 2), the sequences of which belong to a 130 kDa, leucine-rich protein named LRP130 (also named LRPPRC, Swissprot accession

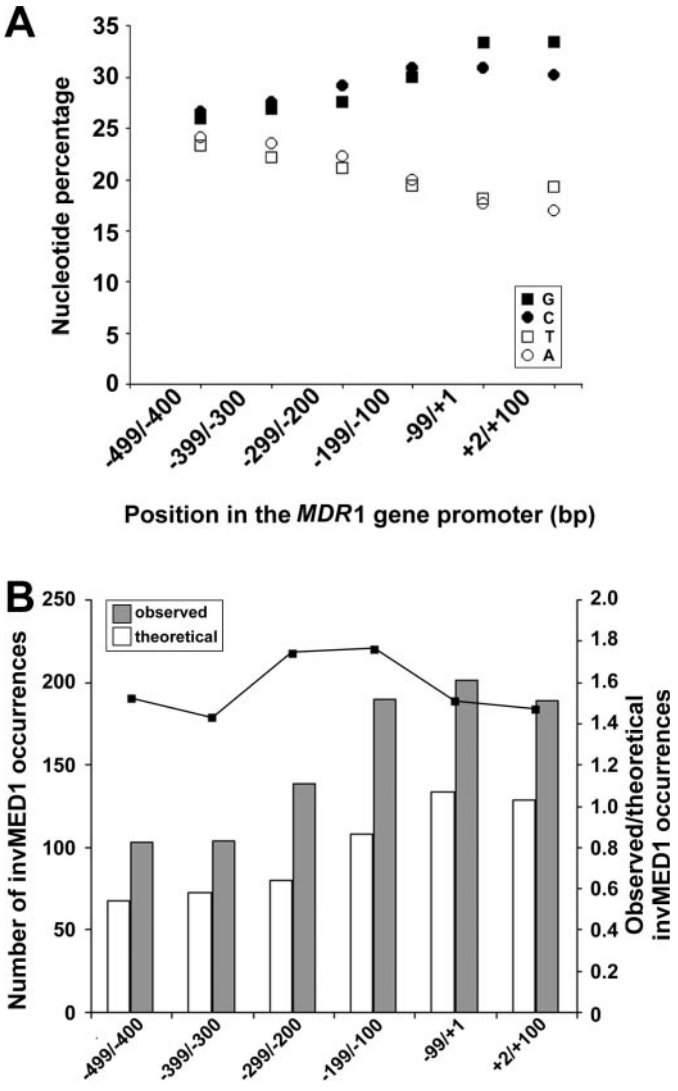

Figure 3. Distribution of A, C, G and T nucleotides in the promoter region of 609 human genes between −499 and +100 bp (**A**), and frequency of the invMED1 hexanucleotide (**B**). The distribution of the 4 nt is expressed as a percentage in each promoter window of 100 nt (A). Both theoretical and observed frequencies of the invMED1 hexanucleotide (white and gray bars, respectively) are reported for each window of 100 nt (B). The right-hand scale of (B) represents the observed/theoretical frequency ratio of the invMED1 occurrence for the same 100 bp windows. Observed invMED1 DNA occurrences concern the 805 GGGAGC hexanucleotides contained in the −499/+100 region of the 609 human gene promoters scanned from the Eukaryotic Promoter Databank, as explained in the text.

no. P42704) (33). The fragments analyzed covered 14.1% of the 1273 residues spanning the entire LRP130 sequence.

To verify that the invMED1 binding factor actually contained LRP130, an EMSA experiment was carried out with the αF-N anti-LRP130 monoclonal antibody. The supershift obtained suggests that LRP130 was directly involved in the binding to invMED1 *in vitro* (Figure 6A). Moreover, LRP130 was effectively eluted from DNA-affinity chromatography experiments with DNA reproducing repeats of the invMED1 sequence. This result was demonstrated by mass spectrometry analysis of the major protein band revealed by silver staining of an SDS–PAGE experiment performed with the eluted fractions (Figure 6B).

Role of the invMED1 DNA sequence in the transcriptional activity of the *MDR*1 and *MVP* gene promoters

To test the role of the invMED1 sequence in the *MDR*1 gene promoter, transient transfections of CEM cells with reporter plasmid constructs were carried out. The constructs tested contained either a full-length *MDR*1 promoter or a promoter in which the invMED1 sequence was deleted. As shown in Figure 7A, deletion of the invMED1 sequence reduced the relative transcriptional activity by ∼60%. Therefore, the invMED1 sequence appears to be a positive regulatory element of the *MDR*1 gene promoter.

To support this result we extended this approach to the endogenous *MDR*1 gene in resistant CEM/VLB5 cells that had been transfected with a phosphorothioate-modified ODN6 decoy reproducing the invMED1 element. Transcriptional decoys are short, double-stranded ODNs reproducing a transcriptional element. When they are introduced in high quantities in the cell, such ODNs are thought to lure the specific nuclear factor (or members of the factor family) that naturally binds their sequence (34,35).

Modulation of the presence of *MDR*1 mRNA induced by the transcriptional decoy was recorded to test the functional effect of the invMED1 element on expression of the endogenous *MDR*1 gene. Figure 7B shows a significant decrease in the expression of *MDR*1 gene transcripts 3 days after transfer of the specific decoy. These results strongly suggest an activating role of invMED1 on the endogenous *MDR*1 gene. In addition, they confirm our previous finding that the 12mer ODN (ODN12) used as a transcriptional decoy for the human *MDR*1 gene promoter decreased the viability of resistant CEM/VLB0.45 cells in the presence of vinblastine (25).

In order to evaluate the impact of the invMED1 DNA sequence on the transcriptional activity of endogenous *MDR*1 and *MVP* genes-expressing cells, we used the transcriptional decoy strategy in the human IPC227 ciliary body melanoma cell line, which co-expresses both MDR-related genes. We transfected phosphorothioate-modified, double-stranded ODN6 reproducing the invMED1 element sequence in the IPC227 cell line. Three days after transfection, cells were analyzed for their relative *MDR*1 and *MVP* transcript contents. After RT–PCR, quantification of specific PCR products was done by laser scan densitometry. Figure 7C shows that an invMED1 decoy (ODN6) induced a marked decrease of the expression of *MDR*1 and *MVP* transcripts whereas the use of a decoy bearing a G/A substitution at position 3 (ODN6M) did not produce any significant effect on the level of both transcripts. These results demonstrate that the invMED1 element affects the activation of the endogenous *MDR*1 and *MVP* genes.

Role of LRP130 in the transcriptional activity of the human *MDR*1 and *MVP* gene promoters

To examine the role of LRP130 in the *MDR*1 gene expression we used a specific siRNA directed against LRP130, which induced a 60% inhibition of the transcriptional activity of the full-length *MDR*1 gene promoter (Figure 8). From a functional point of view, this result indicates that LRP130 exerts a positive transcriptional control on the *MDR*1 gene. On the other hand, the same siRNA did not exert any significant transcriptional control over the invMED1-deleted construct

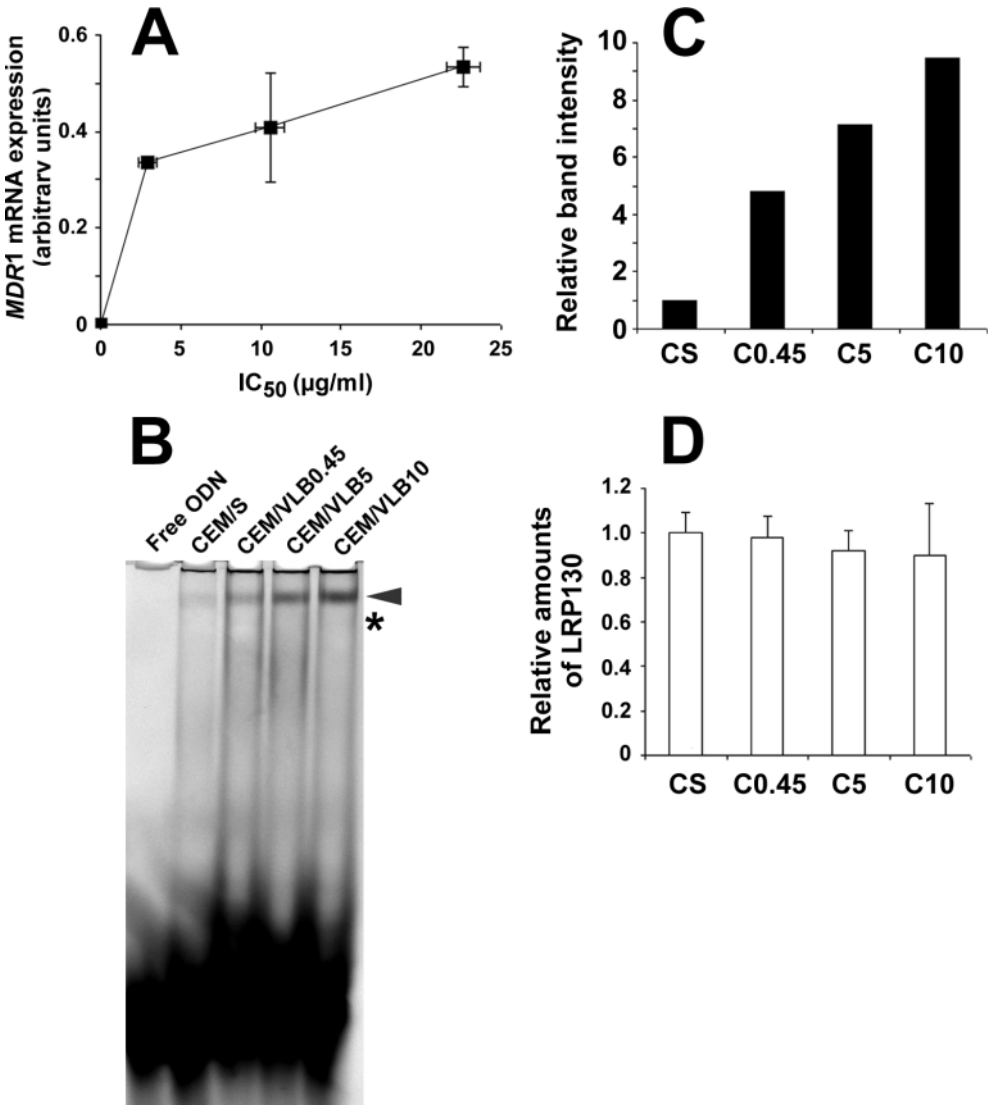

Figure 4. Interaction of the invMED1 binding factor with invMED1 as a function of degree of chemoresistance. (**A**) Presence of *MDR*1 mRNA in CEM cells as a function of IC_{50} of sensitive and resistant cell lines. RT–PCR products from *MDR*1 and β-actin gene transcripts were separated by electrophoresis and quantified by fluorescence analysis after staining of the gel with SYBR-Green. Expression of *MDR*1 transcripts was normalized to that of β-actin transcripts. Results of four experiments ± SD are presented. (**B**) EMSA analysis with 10 µg of nuclear extracts from sensitive (CEM/S) and resistant (CEM/VLB0.45, CEM/VLB5 and CEM/VLB10) cells, and labeled ODN6. (**C**) The relative band intensity for ODN6–nuclear factor complex was analyzed using a blot evaluation software after background correction for which a sample was withdrawn at the level of the asterisk in (B). Band intensity was arbitrarily set to 1 in the case of CEM/S nuclear extracts. One typical experiment is presented. (**D**) LRP130 production in sensitive and resistant CEM cell lines. Of the total protein extracts, 10 µg from each sensitive and resistant CEM cells were analyzed by western blot using the anti-LRP130 αF-N monoclonal antibody, and the intensity of the related band was quantified by laser scan densitometry. Results of four experiments in quadruplicate ± SD are presented. CS: CEM/S; C0.45: CEM/VLB0.45; C5: CEM/VLB5; C10: CEM/VLB10.

(Figure 8), indicating that the transcriptional control played by LRP130 on the *MDR*1 gene promoter depends on the invMED1 element.

To examine the role of LRP130 in the *MVP* gene expression, we constructed a reporter plasmid containing the *MVP* promoter region. The plasmid was then transiently transfected with or without an siRNA directed against LRP130 into CEM cells, and reporter gene expression levels were measured. As shown in Figure 9, inhibition of LRP130 by an siRNA resulted in an important reduction (>60%) of the reporter gene expression. This suggests that LRP130 exerts a positive effect on the *MVP* gene promoter activity.

To attribute a role to LRP130 in endogenous *MDR*1 and *MVP* genes expression, transient transfections of the human fibrosarcoma HT1080 cell line were performed, using siRNA-producing constructs directed against LRP130 (Figure 10). Three days after transfection, the level of *LRP130* transcripts was significantly reduced. In addition, the *MDR*1 gene was almost totally knocked down, the *MVP* mRNA levels were highly lowered, while the expression of *MRP*1, which does not contain an invMED1 sequence, did not change. This result suggests that LRP130 could up-regulate the transcription of *MDR*1 and *MVP* genes, although we cannot exclude possible post-transcriptional effects on their mRNAs.

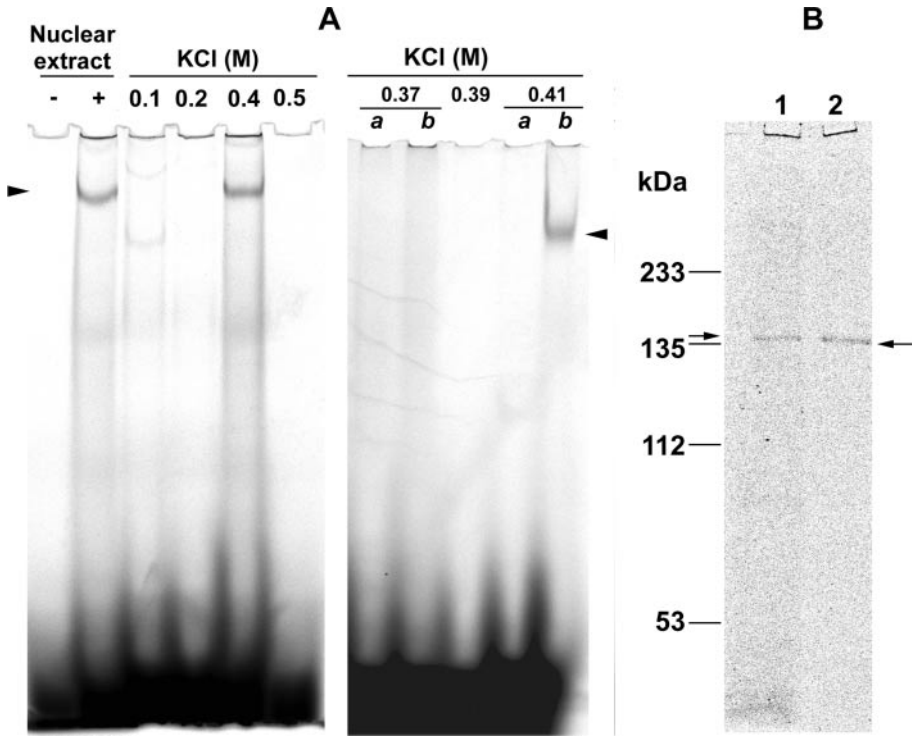

Figure 5. Pre-purification analysis of the invMED1 binding factor. (**A**) Total nuclear proteins were prepared, separated by heparin–sepharose chromatography and eluted by stepwise increasing KCl concentrations from 0.1 to 0.5 M, as indicated. They were further analyzed for binding to ODN6 by EMSA. Lanes *a* and *b* for both 0.37 M and 0.41 M KCl contain the early and late peaks which were eluted at these two KCl concentrations. Arrowheads show the band of interest. (**B**) UV cross-linking of cyanine-5-labeled ODN6 and total nuclear proteins (lane 1) or 0.41 M KCl-eluted fraction (lane 2). SDS–PAGE was further performed and the cyanine-5 labeling was detected by laser scan densitometry. The marked band of interest was cut out and further analyzed by MALDI-TOF and MS–MS spectrometry.

Table 2. Amino acid sequences and analysis of peptides identified by mass spectrometry

Peptide sequence	Length	Position on LRP130
SCGSLLPELK	10	8–17
LGAVYDVSHYNALLKVYLQNE-YKFSPTDFLAKMEEANIQPNR	42	35–76
NVQGIIEILK	10	333–342
SNTLPISLQSIRSSLLLGFR	20	409–428
IPENIYR	7	497–503
IHDVLCK	7	737–743
LQWFCDRCVANNQVETLEKLVELTQK	26	802–827
LLAEILR	7	874–880
GAYDIFLNAK	10	929–938
GFTLNDAANSR	11	978–988
TVLDQQQTPSR	11	1008–1018
LDDLFLK	7	1230–1236

DISCUSSION

MDR-related genes are key components of the cell and tissue drug defense networks. Several studies have shown that *MDR*1 expression is regulated at the transcriptional level by a number of *cis*-elements (36). However, the molecular mechanisms of human *MDR*1 gene regulation are not yet well defined. In a previous study, we used a 12 bp transcriptional decoy reproducing the −108/−97 region of the human *MDR*1 gene; we demonstrated its ability to reduce the *MDR*1 gene transcription, thus resulting in the chemosensitization of resistant CEM/VLB0.45 cells to treatment with vinblastine, and

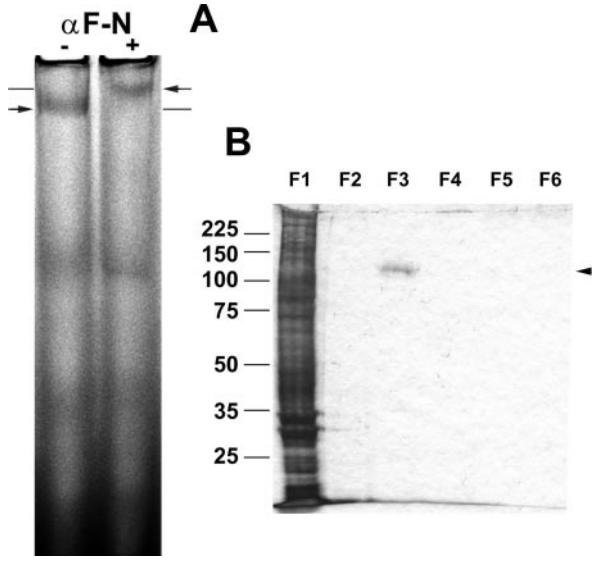

Figure 6. Involvement of LRP130 in the invMED1-dependent transcription of the *MDR*1 gene promoter. (**A**) Presence of the LRP130 protein in the invMED1 binding factor. EMSA supershift analysis with CEM/VLB5 nuclear extracts and ODN6 alone (minus sign) or in the presence of the α-FN anti-LRP130 monoclonal antibody (plus sign). Arrows indicate the relative positions of the bands of interest. (**B**) Nuclear extracts from CEM/VLB5 cells were separated by invMED1 DNA-affinity chromatography. Protein contents from fraction F1 (injection of nuclear extracts in the column), fraction F2 (washing steps of the column), fractions F3 to F5 (elution with 0.5, 1 and 2 M KCl, respectively), and fraction F6 (final washing elution), were analyzed by SDS–PAGE followed by silver staining.

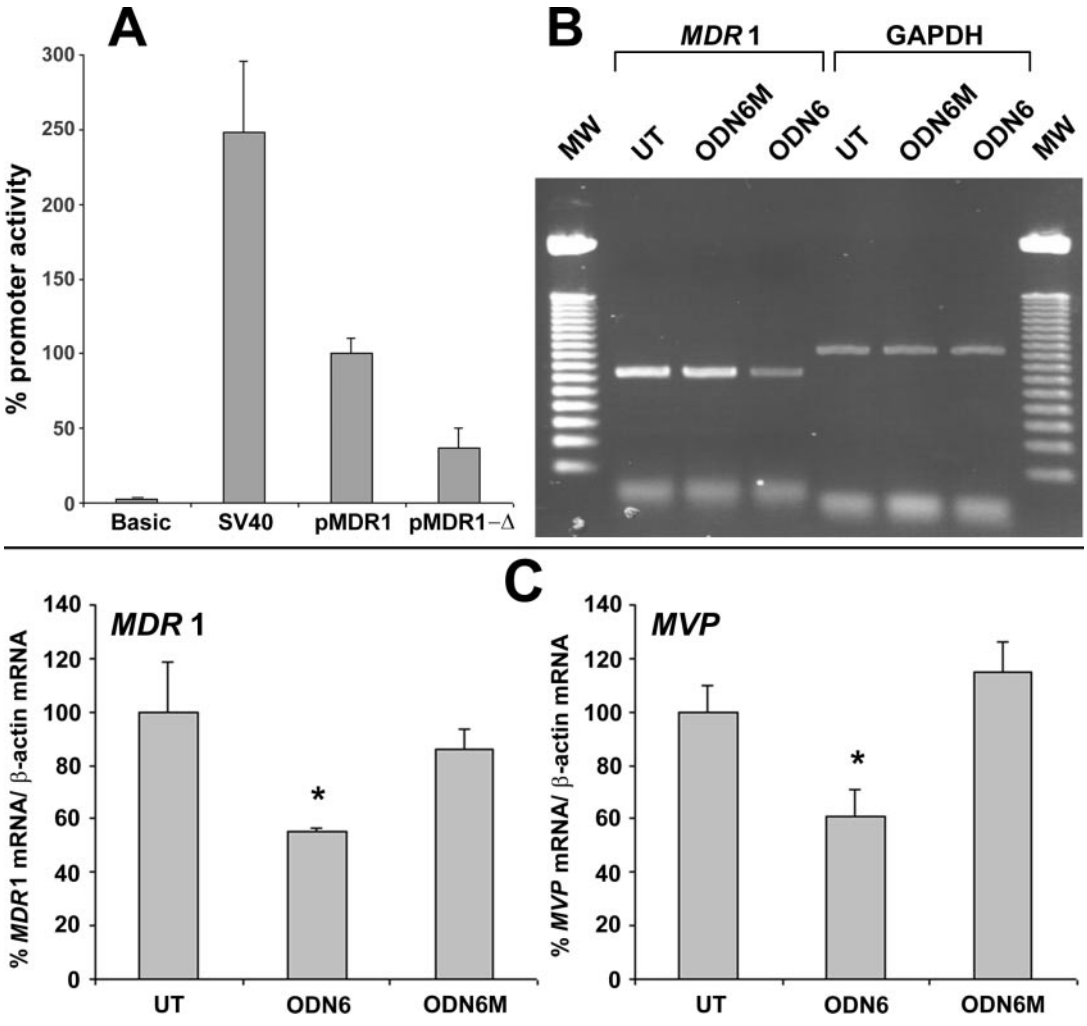

Figure 7. Role of invMED1 in the transcriptional activity of MDR-related gene promoters. (**A** and **B**) Effect of invMED1 decoys on *MDR*1-expressing CEM cells. (A) CEM cells were transiently transfected with plasmid constructs which contained either a wild *MDR*1 promoter fragment (pGL2-h*MDR*1, pMDR1) or a promoter fragment in which invMED1 had been deleted (pGL2-h*MDR*1-ΔinvMED1, pMDR1-Δ). Control promoter activity is represented by the pGL2-control vector (SV40). The reporter luciferase activity was normalized to the β-galactosidase activity (pSV-β-Galactosidase) as internal standard. The data ($n = 4$) are the means ± SD of quadruplicate experiments. (B) Decoy of invMED1-binding nuclear protein(s) to test the effect of the invMED1 element on the expression of endogenous *MDR*1 gene. Chemoresistant CEM/VLB5 cells were transfected either with a decoy reproducing the invMED1 sequence (ODN6) or a decoy bearing a G/A substitution at position 3 (ODN6M), or were not transfected (UT). Three days later, total mRNAs were collected and RT–PCR experiments were performed to reveal *MDR*1 and *GAPDH* transcripts. MW: molecular weight marker (50 bp DNA Step Ladder, Promega). (**C**) Effect of invMED1 decoys on *MDR*1 and *MVP* transcripts in the IPC227 cell line. Expression of *MDR*1 and *MVP* transcripts was evaluated by RT–PCR and is presented relative to the β-*actin* transcript expression. Transcript levels in untransfected cells are set to 100%. Electrophoresis gels were stained with SYBR-Green. PCR products were revealed by laser scan densitometry and quantified with the Image QuaNT analysis software. UT: untransfected cells; ODN6: decoy reproducing the invMED1 GGGAGC sequence; ODN6M: double-stranded decoy with the 5′-GGAAGC sequence bearing a G→A substitution at position 3. The data are the means ± SD of triplicate experiments (asterisk: means significantly different with $p < 0.01$).

showed the presence of a *cis*-element in the −108/−97 region (25,26). In this study, screening of pre-selected sequences by gel mobility shift assays allowed us to determine the precise boundaries of the nuclear factor-binding site at position −105 to −100, which we called invMED1 (Figure 1).

Sixteen human, mouse and rat MDR-related gene promoters have been cloned to date. We showed that seven of them possess an invMED1 sequence (Table 1). The position similarities of the invMED1 elements found, particularly in the −160/−100 region (and more precisely −105/−100 and −148/−143 regions for *MDR*1 and *MVP*, respectively), suggested a possible functional role. Directed deletion experiments and cell transfection with transcriptional decoys demonstrated that this sequence is required for the *MDR*1 (Figure 7A) and *MVP* promoters' activity (Figure 9). Besides the MDR-related genes, the analysis of 1869 human promoters deposited in the Eukaryotic Promoter Databank shows that only 32.5% have at least one occurrence of the GGGAGC hexanucleotide. Although the frequency of the latter increases with the increased G and C nucleotides between −499 and +100 bp, our analysis showed that the observed frequency exceeded 1.8 times the theoretical frequency in the −299/−100 bp segment. The significant presence of the hexanucleotide in this area suggests its biological utility and is in all the

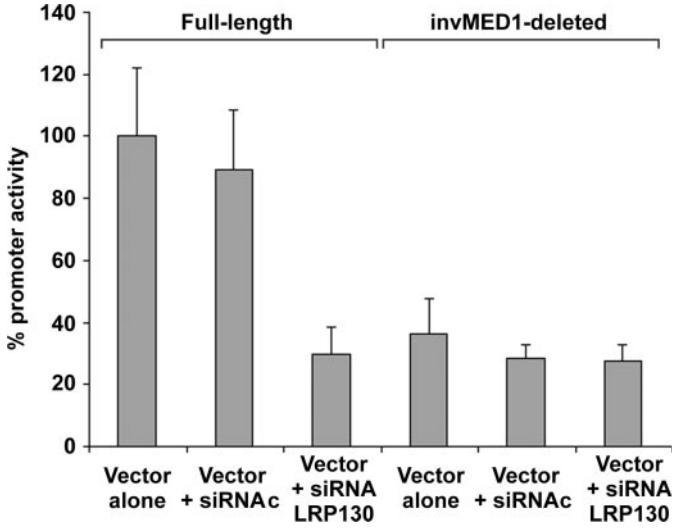

Figure 8. Effect of the reduced *LRP130* gene expression on the transcriptional activity of the invMED1 element in the *MDR*1 promoter. CEM/VLB5 cells were transiently transfected with either the full-length *MDR*1 promoter or the promoter in which invMED1 had been deleted, as described in the legend to Figure 3A. The resulting vectors were co-transfected with either a control construct (siRNAc) or a construct expressing an siRNA directed against LRP130 (siRNA LRP130), or not co-transfected (vector alone). The data are the means of triplicate experiments ± SD.

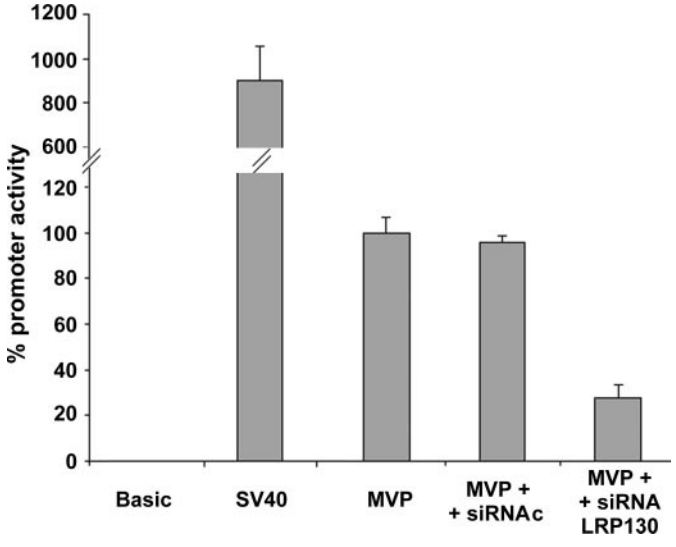

Figure 9. Role of LRP130 in the transcriptional activity of the *MVP* gene promoter. CEM cells were transiently transfected with a full-length human *MVP* promoter (pGL2-MVP1.9) and co-transfected or not with either a control construct (siRNAc) or a construct expressing an siRNA directed against LRP130 (siRNA LRP130). Enzymatic activity provided by the pGL2-MVP1.9 construct alone was arbitrarily set to 100%. The data are the means of triplicate experiments ± SD.

cases consistent with the position of the functional invMED1 element in the MDR-related genes that we studied. The extended analysis to the rodent gene promoters of the Eukaryotic Promoter Database confirmed that the −299/−100 region displayed a frequency for the observed GGGAGC occurrence that was significantly higher than the theoretical

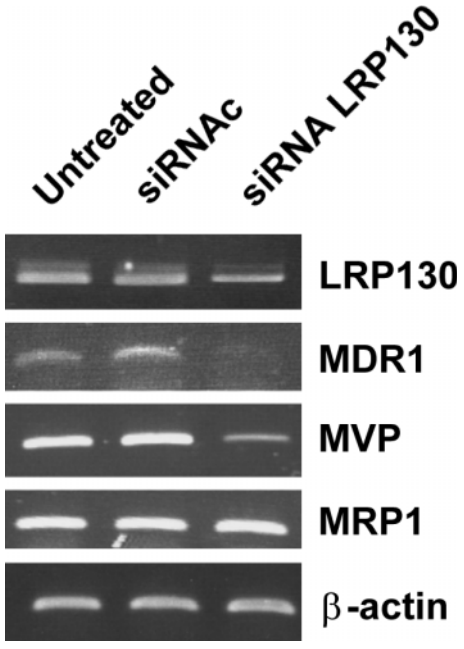

Figure 10. Role of LRP130 in the endogenous transcriptional activity of *MDR*1 and *MVP* genes. HT1080 cells were transiently transfected or not with either the siRNA control construct (siRNAc) or the construct expressing an siRNA directed against LRP130 (siRNA LRP130).

one, suggesting its possible involvement in yet unknown gene regulatory processes.

A search for potential invMED1 binding protein candidates was carried out using promoter databases such as TRANSFAC® professional. No known or described nuclear factor was retrieved. We therefore performed a series of experiments to further identify potential candidates. Our results revealed the presence of LRP130 in the invMED1 binding nuclear complex (Table 2). We performed *in vitro* and *in cellulo* experiments to confirm the involvement of the LRP130 protein in the invMED1 transcriptional activity of the *MDR*1 gene (Figures 6 and 8). The LRP130 protein, also called LRPPRC, is a leucine-rich protein of ∼130 kDa (37), the function of which is still under investigation. This protein has been reported to bind to nuclear (38) and mitochondrial (39) polyadenylated RNAs, possibly being involved in their transport. Mutations in its gene sequence have also been involved in the natural history of the Leigh syndrome, French–Canadian type, a human cytochrome *c* oxidase deficiency (40). LRP130 seems to play several other intracellular roles, which are currently under investigation, like cytoskeletal organization, vesicular trafficking and chromosome activity (41,42). Here we bring the proof of a new functionality that this protein exerts in the transcriptional regulation of two MDR-related genes, *MDR*1 and *MVP*. Interestingly, our data are supported by two-hybrid experiments, which suggest a possible link between LRP130 and some factors involved in the transcriptional machinery (41).

The presence of an invMED1 sequence in multiple mammalian MDR-related genes suggests its possible link to the MDR phenotype. We investigated the invMED1-binding capacity of the LRP130 factor as a function of the chemoresistance level of CEM cell lines. The correlation observed between the level of expression of the MDR phenotype, the

*MDR*1 mRNA level and the invMED1-binding intensity (Figure 4), suggests that the transcriptional effect of the invMED1/LRP130 couple depends on the cellular level of the MDR phenotype. Even though the invMED1/LRP130 complex formation increased with the chemoresistance level, the total amount of LRP130 available in both sensitive and resistant cells remained almost identical in all the cell lines. This is probably due to the fact that the total amount of LRP130 in both sensitive and resistant cells is always largely above the very small quantity that is needed to form the invMED1/LRP130 complex.

Because of its involvement in the co-regulation of *MDR*1 and *MVP* genes, as we have shown in two different human cancer cell lines (Figure 7C and 10), and possibly of other MDR-related genes, the invMED1/LRP130 complex may be regarded as a central element in the hypothesis of a functional multidrug resistance mechanism in which drugs could effectively be conveyed inside the cytoplasm by vaults and be expelled out of the cell by membrane pumps (14). The involvement of LRP130 in several cellular mechanisms as well as the very weak fraction implicated in the activator complex allow the prediction that its knocking down may be harmful for cellular survival. Therefore, to be effective and not to affect the other cellular functions of LRP130, chemosensitization of MDR cells should consequently pass by the specific invalidation of the invMED1/LRP130 complex formation.

ACKNOWLEDGEMENTS

We are grateful to Dr Hitoshi Nakagama (National Cancer Center Research Institute, Tokyo, Japan) for his kind gift of anti-LRP130 αF-N antibody, Dr Patricia Rousselle (IBCP-CNRS) for providing us with the skin fibrosarcoma HT-1080 cell line and NHF primary cultures, Dr Susan E. Kane for her kind gift of the *MDR*1-transduced NIH80 cell line, Pr François Amalric and Dr Bernard Monsarrat (IPBS-CNRS, Toulouse) for mass spectrometry analyses, and Dr David Hulmes (IBCP-CNRS) for helpful discussions. This work was supported by grants from Ligue contre le Cancer (Comité du Rhône, Comité de la Loire, Comité de la Saône et Loire, Comité National); Retina France; Fondation Mérieux, Fondation pour la Recherche Médicale and Association pour la Recherche contre le Cancer (ARC).

REFERENCES

1. Cole,S.P., Bhardwaj,G., Gerlach,J.H., Mackie,J.E., Grant,C.E., Almquist,K.C., Stewart,A.J., Kurz,E.U., Duncan,A.M. and Deeley,R.G. (1992) Overexpression of a transporter gene in a multidrug-resistant human lung cancer cell line. *Science*, **258**, 1650–1654.
2. Taniguchi,S., Mochida,Y., Uchiumi,T., Tahira,T., Hayashi,K., Takagi,K., Shimada,M., Maehara,Y., Kuwano,H., Kono,S. *et al.* (2003) Genetic polymorphism at the 5′ regulatory region of multidrug resistance 1 (MDR1) and its association with interindividual variation of expression level in the colon. *Mol. Cancer Ther.*, **2**, 1351–1359.
3. Kool,M., van der Linden,M., de Haas,M., Scheffer,G.L., de Vree,J.M., Smith,A.J., Jansen,G., Peters,G.J., Ponne,N., Scheper,R.J. *et al.* (1999) MRP3, an organic anion transporter able to transport anti-cancer drugs. *Proc. Natl Acad. Sci. USA*, **96**, 6914–6919.
4. Schuetz,J.D., Connelly,M.C., Sun,D., Paibir,S.G., Flynn,P.M., Srinivas,R.V., Kumar,A. and Fridland,A. (1999) MRP4: a previously unidentified factor in resistance to nucleoside-based antiviral drugs. *Nature Med.*, **5**, 1048–1051.
5. Wijnholds,J., Mol,C.A., van Deemter,L., de Haas,M., Scheffer,G.L., Baas,F., Beijnen,J.H., Scheper,R.J., Hatse,S., De Clercq,E. *et al.* (2000) Multidrug-resistance protein 5 is a multispecific organic anion transporter able to transport nucleotide analogs. *Proc. Natl Acad. Sci. USA*, **97**, 7476–7481.
6. Doyle,L.A., Yang,W., Abruzzo,L.V., Krogmann,T., Gao,Y., Rishi,A.K. and Ross,D.D. (1998) A multidrug resistance transporter from human MCF-7 breast cancer cells. *Proc. Natl Acad. Sci. USA*, **95**, 15665–15670.
7. Smith,A.J., van Helvoort,A., van Meer,G., Szabo,K., Welker,E., Szakacs,G., Varadi,A., Sarkadi,B. and Borst,P. (2000) MDR3 P-glycoprotein, a phosphatidylcholine translocase, transports several cytotoxic drugs and directly interacts with drugs as judged by interference with nucleotide trapping. *J. Biol. Chem.*, **275**, 23530–23539.
8. Nooter,K., Sonneveld,P., Janssen,A., Oostrum,R., Boersma,T., Herweijer,H., Valerio,D., Hagemeijer,A. and Baas,F. (1990) Expression of the mdr3 gene in prolymphocytic leukemia: association with cyclosporin-A-induced increase in drug accumulation. *Int. J. Cancer*, **45**, 626–631.
9. Herweijer,H., Sonneveld,P., Baas,F. and Nooter,K. (1990) Expression of mdr1 and mdr3 multidrug-resistance genes in human acute and chronic leukemias and association with stimulation of drug accumulation by cyclosporine. *J. Natl Cancer Inst.*, **82**, 1133–1140.
10. Scheffer,G.L., Wijngaard,P.L., Flens,M.J., Izquierdo,M.A., Slovak,M.L., Pinedo,H.M., Meijer,C.J., Clevers,H.C. and Scheper,R.J. (1995) The drug resistance-related protein LRP is the human major vault protein. *Nature Med.*, **1**, 578–582.
11. Kedersha,N.L., Miquel,M.C., Bittner,D. and Rome,L.H. (1990) Vaults. II. Ribonucleoprotein structures are highly conserved among higher and lower eukaryotes. *J. Cell Biol.*, **110**, 895–901.
12. Hamill,D.R. and Suprenant,K.A. (1997) Characterization of the sea urchin major vault protein: a possible role for vault ribonucleoprotein particles in nucleocytoplasmic transport. *Dev. Biol.*, **190**, 117–128.
13. Abbondanza,C., Rossi,V., Roscigno,A., Gallo,L., Belsito,A., Piluso,G., Medici,N., Nigro,V., Molinari,A.M., Moncharmont,B. *et al.* (1998) Interaction of vault particles with estrogen receptor in the MCF-7 breast cancer cell. *J. Cell Biol.*, **141**, 1301–1310.
14. Mossink,M.H., van Zon,A., Scheper,R.J., Sonneveld,P. and Wiemer,E.A. (2003) Vaults: a ribonucleoprotein particle involved in drug resistance? *Oncogene*, **22**, 7458–7467.
15. den Boer,M.L., Pieters,R., Kazemier,K.M., Rottier,M.M., Zwaan,C.M., Kaspers,G.J., Janka-Schaub,G., Henze,G., Creutzig,U., Scheper,R.J. *et al.* (1998) Relationship between major vault protein/lung resistance protein, multidrug resistance-associated protein, P-glycoprotein expression, and drug resistance in childhood leukemia. *Blood*, **91**, 2092–2098.
16. Den Boer,M.L., Pieters,R., Kazemier,K.M., Janka-Schaub,G.E., Henze,G. and Veerman,A.J. (1999) Relationship between the intracellular daunorubicin concentration, expression of major vault protein/lung resistance protein and resistance to anthracyclines in childhood acute lymphoblastic leukemia. *Leukemia*, **13**, 2023–2030.
17. Goasguen,J.E., Lamy,T., Bergeron,C., Ly Sunaram,B., Mordelet,E., Gorre,G., Dossot,J.M., Le Gall,E., Grosbois,B., Le Prise,P.Y. *et al.* (1996) Multifactorial drug-resistance phenomenon in acute leukemias: impact of P170-MDR1, LRP56 protein, glutathione-transferases and metallothionein systems on clinical outcome. *Leuk Lymphoma*, **23**, 567–576.
18. List,A.F., Spier,C.S., Grogan,T.M., Johnson,C., Roe,D.J., Greer,J.P., Wolff,S.N., Broxterman,H.J., Scheffer,G.L., Scheper,R.J. *et al.* (1996) Overexpression of the major vault transporter protein lung-resistance protein predicts treatment outcome in acute myeloid leukemia. *Blood*, **87**, 2464–2469.
19. Borg,A.G., Burgess,R., Green,L.M., Scheper,R.J. and Yin,J.A. (1998) Overexpression of lung-resistance protein and increased P-glycoprotein function in acute myeloid leukaemia cells predict a poor response to chemotherapy and reduced patient survival. *Br. J. Haematol.*, **103**, 1083–1091.
20. Filipits,M., Pohl,G., Stranzl,T., Suchomel,R.W., Scheper,R.J., Jager,U., Geissler,K., Lechner,K. and Pirker,R. (1998) Expression of the lung resistance protein predicts poor outcome in de novo acute myeloid leukemia. *Blood*, **91**, 1508–1513.
21. Schneider,J., Gonzalez-Roces,S., Pollan,M., Lucas,R., Tejerina,A., Martin,M. and Alba,A. (2001) Expression of LRP and MDR1 in locally advanced breast cancer predicts axillary node invasion at the time of

rescue mastectomy after induction chemotherapy. *Breast Cancer Res*., **3**, 183–191.
22. Ogretmen,B. and Safa,A.R. (2000) Identification and characterization of the MDR1 promoter-enhancing factor 1 (MEF1) in the multidrug resistant HL60/VCR human acute myeloid leukemia cell line. *Biochemistry*, **39**, 194–204.
23. Zhong,X. and Safa,A.R. (2004) RNA helicase A in the MEF1 transcription factor complex upregulates the MDR1 gene in multidrug resistant cancer cells. *J. Biol. Chem*., **279**, 17134–17141.
24. Synold,T.W., Dussault,I. and Forman,B.M. (2001) The orphan nuclear receptor SXR coordinately regulates drug metabolism and efflux. *Nature Med*., **7**, 584–590.
25. Marthinet,E., Divita,G., Bernaud,J., Rigal,D. and Baggetto,L.G. (2000) Modulation of the typical multidrug resistance phenotype by targeting the MED-1 region of human MDR1 promoter. *Gene Ther*., **7**, 1224–1233.
26. Labialle,S., Gayet,L., Marthinet,E., Rigal,D. and Baggetto,L.G. (2002) Transcriptional regulation of the human MDR1 gene at the level of the inverted MED-1 promoter region. *Ann. N.Y. Acad. Sci*., **973**, 468–471.
27. Morris,M.C., Vidal,P., Chaloin,L., Heitz,F. and Divita,G. (1997) A new peptide vector for efficient delivery of oligonucleotides into mammalian cells. *Nucleic Acids Res*., **25**, 2730–2736.
28. Dong,M., Penin,F. and Baggetto,L.G. (1996) Efficient purification and reconstitution of P-glycoprotein for functional and structural studies. *J. Biol. Chem*., **271**, 28875–28883.
29. Jackson,S.P. (2003) Identification and characterization of eukaryotic transcription factors. In Hames,B.D. and Higgins,S.J. (eds), *Gene Transcription: A Practical Approach*. IRL Press, Oxford, UK, pp. 189–242.
30. Bradford,M.M. (1976) A rapid and sensitive method for the quantitation of microgram quantities of protein utilizing the principle of protein-dye binding. *Anal. Biochem*., **72**, 248–254.
31. Laemmli,U.K. (1970) Cleavage of structural proteins during the assembly of the head of bacteriophage T4. *Nature*, **227**, 680–685.
32. Penin,F., Godinot,C. and Gautheron,D.C. (1984) Two-dimensional gel electrophoresis of membrane proteins using anionic and cationic detergents. Application to the study of mitochondrial F0-F1-ATPase. *Biochim. Biophys. Acta*, **775**, 239–245.
33. Combates,N.J., Rzepka,R.W., Chen,Y.N. and Cohen,D. (1994) NF-IL6, a member of the C/EBP family of transcription factors, binds and trans-activates the human MDR1 gene promoter. *J. Biol. Chem*., **269**, 29715–29719.
34. Bielinska,A., Shivdasani,R.A., Zhang,L.Q. and Nabel,G.J. (1990) Regulation of gene expression with double-stranded phosphorothioate oligonucleotides. *Science*, **250**, 997–1000.
35. Lee,Y.N., Park,Y.G., Choi,Y.H., Cho,Y.S. and Cho-Chung,Y.S. (2000) CRE-transcription factor decoy oligonucleotide inhibition of MCF-7 breast cancer cells: cross-talk with p53 signaling pathway. *Biochemistry*, **39**, 4863–4868.
36. Labialle,S., Gayet,L., Marthinet,E., Rigal,D. and Baggetto,L.G. (2002) Transcriptional regulators of the human multidrug resistance 1 gene: recent views. *Biochem. Pharmacol*., **64**, 943–948.
37. Hou,J., Wang,F. and McKeehan,W.L. (1994) Molecular cloning and expression of the gene for a major leucine-rich protein from human hepatoblastoma cells (HepG2). *In Vitro Cell Dev. Biol. Anim*., **30A**, 111–114.
38. Mili,S., Shu,H.J., Zhao,Y. and Pinol-Roma,S. (2001) Distinct RNP complexes of shuttling hnRNP proteins with pre-mRNA and mRNA: candidate intermediates in formation and export of mRNA. *Mol. Cell. Biol*., **21**, 7307–7319.
39. Mili,S. and Pinol-Roma,S. (2003) LRP130, a pentatricopeptide motif protein with a noncanonical RNA-binding domain, is bound *in vivo* to mitochondrial and nuclear RNAs. *Mol. Cell. Biol*., **23**, 4972–4982.
40. Mootha,V.K., Lepage,P., Miller,K., Bunkenborg,J., Reich,M., Hjerrild,M., Delmonte,T., Villeneuve,A., Sladek,R., Xu,F. *et al*. (2003) Identification of a gene causing human cytochrome *c* oxidase deficiency by integrative genomics. *Proc. Natl Acad. Sci. USA*, **100**, 605–610.
41. Liu,L. and McKeehan,W.L. (2002) Sequence analysis of LRPPRC and its SEC1 domain interaction partners suggests roles in cytoskeletal organization, vesicular trafficking, nucleocytosolic shuttling, and chromosome activity. *Genomics*, **79**, 124–136.
42. Liu,L., Amy,V., Liu,G. and McKeehan,W.L. (2002) Novel complex integrating mitochondria and the microtubular cytoskeleton with chromosome remodeling and tumor suppressor RASSF1 deduced by *in silico* homology analysis, interaction cloning in yeast, and colocalization in cultured cells. *In Vitro Cell Dev. Biol. Anim*., **38**, 582–594.